

Pseudoscalar transition form factors and the hadronic light-by-light contribution to the muon $g - 2$

Antoine Gérardin,^a Jana N. Guenther,^{a,b} Lukas Varnhorst^{a,b} and Willem E. A. Verplanke^{a,*} for the Budapest-Marseille-Wuppertal Collaboration

^a*Aix-Marseille Université, Université de Toulon, CNRS, CPT, Marseille, France*

^b*Department of Physics, University of Wuppertal, D-42119 Wuppertal, Germany*

E-mail: willem.verplanke@cpt.univ-mrs.fr, antoine.gerardin@cpt.univ-mrs.fr

We present preliminary results from our calculation of the pseudoscalar transition form factors of the η and η' mesons using staggered quarks on $N_f = 2 + 1 + 1$ gauge ensembles generated by the Budapest-Marseille-Wuppertal collaboration. These transition form factors are an important input for the hadronic light-by-light contribution to the muon ($g - 2$). We first elaborate on the extraction of the masses of the η and η' mesons, that mix under the dynamics of QCD. Thereafter, we show our preliminary results for the pseudoscalar transition form factors, focusing on the η meson in the absence of mixing.

*The 38th International Symposium on Lattice Field Theory, LATTICE2021 26th-30th July, 2021
Zoom/Gather@Massachusetts Institute of Technology*

*Speaker

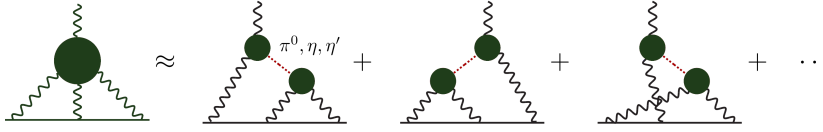


Figure 1: Hadronic light-by-light diagram and its decomposition into the dominant pseudoscalar poles. A wobbly line indicates a photon, the straight line the muon and a blob the non-perturbative hadronic interactions encoded in the pseudoscalar TFF.

1. Introduction

Understanding the discrepancy between the theory calculation and the experimental value of the muon anomalous magnetic moment (a_μ) [1] is one of the most pressing challenges in present-day particle physics. The theoretical error is dominated by the hadronic vacuum polarization (HVP) and the hadronic light-by-light (HLbL) contributions. A recent computation of the leading order HVP by the Budapest-Marseille-Wuppertal (BMW) collaboration has however shed new light on the issue [2]. In particular, it reduces the tension with the experimental value of a_μ .

The HLbL interaction is shown in Figure 1. This contribution results from the scattering of four photons by means of a non-perturbative hadronic interaction. Two model-independent routes to calculate the diagram are nowadays applied, namely the dispersive [3–5] and lattice [6, 7] computations. Crucial input for the dispersive approach are the transition form factors (TFFs) of the π^0 , η and η' mesons, which are directly linked to pseudoscalar pole contributions to the a_μ^{HLbL} . The TFF describes the interaction of one on-shell pseudoscalar meson with two off-shell photons. The pion TFF has already been calculated [8, 9], and we provide here our first results towards a calculation of the η and η' TFFs. Note finally that, in experiment, the η and η' TFFs are difficult to access in the doubly virtual regime, where the photons have the same virtuality, so a theoretical calculation is of particular importance. ETM has already presented preliminary results of a calculation of the η , η' TFFs [10]. The mixing between the two states encumbers the calculation, but only a 20% precision on the contribution to a_μ^{HLbL} is necessary to match future experimental precision [11].

In line with this interest, the second aim of this project is a calculation of the η and η' masses and mixing angles, using staggered quarks. Recent calculations of these quantities have been done using Wilson-Clover quarks [12] and twisted-mass quarks [13], and have shown good correspondence with experiment. The η and η' mesons are interesting particles to simulate, as the large mass of the η' meson is directly related to the non-perturbative dynamics of QCD and the anomaly in the $U(1)_A$ charge symmetry of the QCD Lagrangian [14]. Besides, flavor singlet mesons require the use of disconnected correlators, which are more challenging to compute and couple directly to the sea. The fourth-root trick employed for the sea quarks in staggered lattice QCD simulations has also been questioned [15, 16]. The η' meson is hence of interest, and can therefore provide another hint towards the ability of staggered quarks to reproduce the axial anomaly in the continuum limit.

2. Simulation details

We use $N_f = 2+1+1$ dynamical staggered fermions with four steps of stout smearing generated by the BMW collaboration [2]. These gauge ensembles are at nearly physical pion and kaon mass.

	β	a[fm]	$L/a \times T/a$	# conf
three-point	3.7000	0.1315	32×64	900
two-point	3.8400	0.0952	32×64	1100

Table 1: Summary of two ensembles with lattice spacing, lattice size and number of gauge configurations.

We plan to exploit five different lattice spacings in the available range and consider $L = 3, 4$ and 6 fm boxes for finite-size effect studies. Simulations are performed in the isospin limit where $m_u = m_d \equiv m_\ell$. In Table 1 we summarize the details of the two ensembles used in this preliminary study. The three-point functions have only been computed on the coarse ensemble.

3. η and η' mass

3.1 Mass extraction

The analysis of the $\eta - \eta'$ system starts by the quark model. One introduces an SU(3) octet and singlet field

$$\eta_8(x) = \frac{1}{\sqrt{6}} \left(\bar{u}\gamma_5 u(x) + \bar{d}\gamma_5 d(x) - 2\bar{s}\gamma_5 s(x) \right), \quad (1)$$

$$\eta_0(x) = \frac{1}{\sqrt{3}} \left(\bar{u}\gamma_5 u(x) + \bar{d}\gamma_5 d(x) + \bar{s}\gamma_5 s(x) \right). \quad (2)$$

The $\eta_8(x)$ field is a Goldstone realization of spontaneously broken symmetry group $G_F = U(1)_V \otimes SU(3)_L \otimes SU(3)_R \xrightarrow{SSB} U(1)_V \otimes SU(3)_V$ of the classical QCD Lagrangian. On the other hand, η_0 is the would-be Goldstone boson realization of the $U(1)_A$ charge symmetry, that is broken at the quantum level. Both fields have quantum numbers $J^{PC} = 0^{-+}$, like the π^0 . However, no mixing with the pion occurs in our lattice simulations since we work in the isospin limit.

We consider the matrix of correlators built from the lattice operators O_8, O_0 that interpolate the SU(3) fields

$$\begin{aligned} C(t) &\equiv \begin{pmatrix} \langle O_8(t) O_8^\dagger(0) \rangle & \langle O_8(t) O_0^\dagger(0) \rangle \\ \langle O_0(t) O_8^\dagger(0) \rangle & \langle O_0(t) O_0^\dagger(0) \rangle \end{pmatrix} \\ &= \begin{pmatrix} \frac{1}{3} (C_\ell + 2C_s - 4D_{\ell s} + 2D_{\ell\ell} + 2D_{ss}) & \frac{\sqrt{2}}{3} (C_\ell - D_{\ell s} - D_{ss} - C_s + 2D_{\ell\ell}) \\ \frac{\sqrt{2}}{3} (C_\ell - D_{\ell s} - D_{ss} - C_s + 2D_{\ell\ell}) & \frac{1}{3} (2C_\ell + C_s + 4D_{\ell\ell} + 4D_{\ell s} + D_{ss}) \end{pmatrix}, \quad (3) \end{aligned}$$

where C_q and $D_{qq'}$ are respectively the connected and disconnected correlator for quark flavor $q, q' = \ell, s$ and we have made use of $D_{ls} = D_{sl}$. Notice that the mixing between η_8 and η_0 is made explicit by the non-vanishing off-diagonal terms; furthermore, even in the $SU(3)_F$ limit, the disconnected contributions to $\langle O_0(t) O_0^\dagger(0) \rangle$ do not vanish. Lastly, in this chiral limit, the physical η and η' state correspond exactly to the η_8 and η_0 state.

Masses of the η and η' mesons can then be obtained by solving a Generalized Eigenvalue Problem (GEVP) [17]

$$C(t)v_n(t, t_0) = \lambda_n(t, t_0)C(t_0)v_n(t, t_0). \quad (4)$$

Here $C(t)$ is an $N \times N$ matrix, λ_n are the eigenvalues, v_n are the eigenvectors, t_0/a is a free parameter that is fixed to 1 in this analysis, and $n \in \{1, \dots, N\}$. From the eigenvalues one can define an effective mass that converges to the meson mass at large time

$$E_n^{\text{eff}}(t) = \log \left(\frac{\lambda_n(t, t_0)}{\lambda_n(t+1, t_0)} \right) \xrightarrow{t \rightarrow \infty} m_n, \quad (5)$$

in the region where the backward propagating quarks can be neglected. In the next section we present the lattice operators that interpolate the η, η' states in the staggered quark formalism.

3.2 Staggered mesonic operators

Staggered mesonic operators have been classified by Golterman in [18]. Following the notation of [19], there are two taste-singlet operators that couple directly to the η, η' mesons

$$O_3(x) = \frac{1}{6} \sum_{ijk} \epsilon_{ijk} \bar{\chi}(x) [\eta_i \Delta_i [\eta_j \Delta_j [\eta_k \Delta_k]]] \chi(x) \equiv \bar{\chi}(x) \hat{O}_3 \chi(x), \quad (6)$$

$$O_4(x) = \frac{1}{2} \eta_4(x) [\bar{\chi}(x) \hat{O}_3 \chi_+(x) + \bar{\chi}_+(x) \hat{O}_3 \chi(x)]. \quad (7)$$

Here $\chi(x)$ is a fermionic field and ϵ_{ijk} is the Levi-Civita tensor; the symmetric shift $\Delta_\mu, \chi_+(x)$ and the staggered phase factors $\eta_\mu(n)$ in the convention $n = (x, y, z, t)$ are

$$\Delta_\mu \chi(x) = \frac{1}{2} [U_\mu(x) \chi(x + \hat{\mu}) + U_\mu^\dagger(x - \hat{\mu}) \chi(x - \hat{\mu})], \quad (8)$$

$$\chi_+(x) = U_4(x) \chi(x + \hat{t}), \quad \bar{\chi}_+(x) = \bar{\chi}(x + \hat{t}) U_4^\dagger(x), \quad (9)$$

$$\eta_\mu(n) = (-1)^{\sum_{\nu < \mu} n_\nu}. \quad (10)$$

In the ubiquitous staggered operator notation $\Gamma_D \otimes \Gamma_F$, where Γ_D denotes the Dirac structure, and Γ_F the taste structure, the 3-link operator $O_3(x)$ couples to an axial vector $\gamma_4 \gamma_5 \otimes 1$ and a parity partner scalar meson $1 \otimes \gamma_4 \gamma_5$. The parity partner for the 3-link operator creates an oscillatory behavior in the effective energy for the taste-singlet pion. This makes a trustworthy extraction of the pseudoscalar ground state energies cumbersome. The 4-link operator $O_4(x)$, which is non-local in time, couples to a pseudoscalar $\gamma_5 \otimes 1$ and an exotic state $\gamma_4 \otimes \gamma_4 \gamma_5$. As noted in [19, 20], the coupling to the parity partner state for such an operator is strongly suppressed. Hence, it is our choice of mesonic operator throughout the analysis, also because the separation by an even amount of links allows for a computational trick, as is discussed next.

3.3 Pseudoscalar two-point functions

We apply several noise-reduction tricks to compute the correlation functions effectively. Firstly, we use low-mode averaging (LMA) [21, 22] with $n = 300$ modes in our 4 fm box (and scale modes with the volume of the box). Secondly, we apply all-mode averaging (AMA) [23, 24] for the stochastic part of our estimator. And lastly, we employ a Venkataraman-Kilcup reduction trick [25] for our one-point functions. In this context, it uses the staggered Dirac operator that connects only even and odd sites, together with the 4-link operator which only couples even (odd) and even (odd) sites. This allows one to construct a different pseudoscalar loop estimator that has a decreased

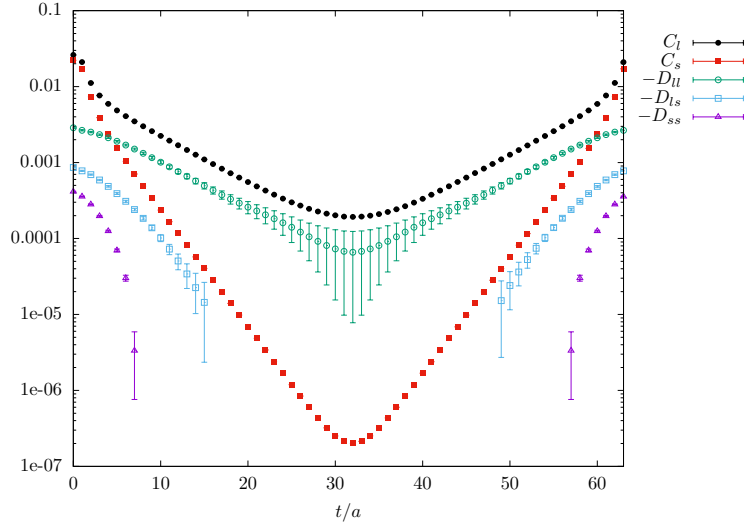


Figure 2: Different connected C_q and disconnected $D_{qq'}$ correlation functions contributing to the η , η' spectroscopic analysis.

variance. As a consequence of all these tricks, we have managed to reach the gauge noise for the two-point disconnected correlation functions. In Figure 2, we show the result for all our correlation functions. Note that we find a good signal for C_ℓ , C_s and $D_{\ell\ell}$, while the signal for the $D_{\ell s}$ and especially the D_{ss} are lost in the noise quickly. This is however not an issue, since the effect of the D_{ss} correlator on the GEVP is extremely small, and to a lesser extent this holds for the $D_{\ell s}$ as well.

3.4 Analysis techniques

Extracting the mass of the η and η' mesons is hindered by the exponential growth of the noise/signal ratio. In fact, by only using a GEVP, the signal of the two mesons is lost before reaching a plateau. Thus, to to circumvent this issue, we apply two analysis techniques. Firstly, we employ a fitting trick to remove excited state contributions in the connected correlator, which was first introduced in this context by ETM [26]. The underlying assumption is that most excited state contamination is found in the connected correlation functions. Since these have a relatively good signal over noise ratio (however not constant, as we work with taste-singlet quantities), it is possible to reliably determine the ground state of these correlators. Connected mesonic correlation functions calculated on a lattice with periodic boundary conditions, assume a spectral decomposition of the form

$$C_q(t) = A_q \left(\exp(-E_q^{(1)} t) + \exp(-E_q^{(1)} (T - t)) \right) + \mathcal{O}(\exp(-E_q^{(2)} t)), \quad q = \ell, s. \quad (11)$$

Fitting C_q to this function in a region where excited states are negligible, one can safely determine the energy E_q and overlap A_q of the ground state. Then one replaces the connected contribution in equation (3) by this one-exponential fit on the whole time range, leaving the disconnected contributions unchanged. If excited state contributions in the disconnected correlators are indeed small, excited states should effectively be removed and a plateau for the effective mass should be reached early in time. Results of applying this method to our data are shown in Figure 3a. We

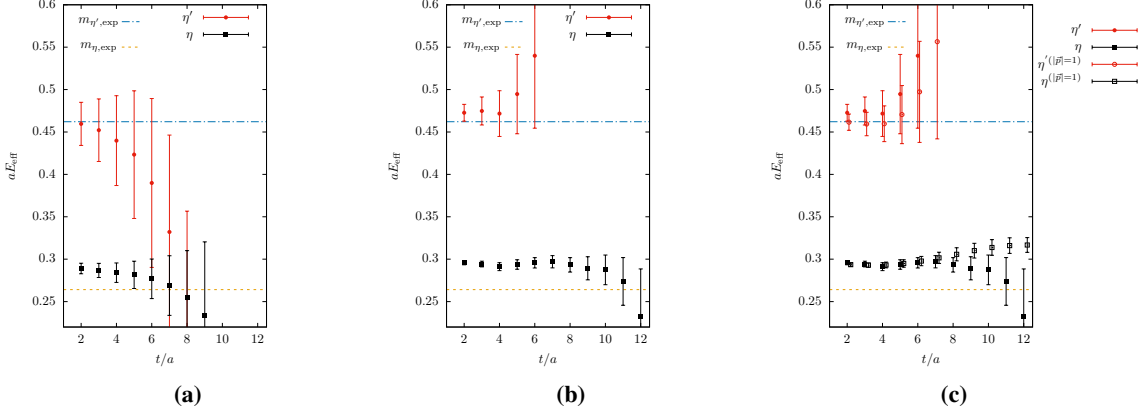


Figure 3: Effective mass plots for three scenarios. Left: after applying method 1 of section 3.4; Middle: Additionally applied method (2); Right: Added the $|\vec{p}| = 1 \cdot \left(\frac{2\pi}{L}\right)$ result. Dashed lines indicate the experimental values of the η and η' masses.

cannot resolve excited states at this stage, but errors are still large, especially for the η' effective mass.

The second trick was first introduced in [13], and results from an analytic understanding of correlation functions in finite volume [27]. In fact, for $\vec{p} = \vec{0}$, disconnected correlation functions in finite volume, do not tend to zero at large time if the topological charge Q isn't correctly sampled. One finds that

$$D_{qq}(t) \stackrel{t \rightarrow \infty}{\sim} \frac{a^5}{T} \left(\chi_t - \frac{Q^2}{V} + \frac{c_4}{2V\chi_t} \right). \quad (12)$$

Here, χ_t is the topological susceptibility and c_4 is the kurtosis of the topological charge. Such a constant shift can be removed by taking a discrete derivative of the matrix of correlators $C(t)$,

$$C(t) \rightarrow C'(t) \equiv C(t) - C(t + \Delta t). \quad (13)$$

This shifted correlation matrix still satisfies a GEVP with $\Delta t/a$ as a free parameter. Aside of removing this constant shift, it also helps reducing correlations between time-slices and hence improves the point error. In Figure 3b we show the result of applying this method to our data, alongside with the first trick, and see that now a plateau is found for η and η' and errors are reduced drastically. Further, in Figure 3c we show the result for our correlation functions which carry one unit of momentum. The errors are slightly smaller and the data are compatible with $\vec{p} = \vec{0}$, motivating a use of both kinematic frames in future analyses. Lastly, we observe a mild discretization effect on the η' meson, while it's of the order of 10% for the η meson.

4. Pseudoscalar transition form factors

In Minkowski space-time, the TFF for a pseudoscalar meson $\mathcal{F}_{p\gamma^*\gamma^*}(q_1^2, q_2^2)$ is defined by the following matrix elements $M_{\mu\nu}$

$$M_{\mu\nu}(p, q_1) = i \int d^4x e^{iq_1 \cdot x} \langle \Omega | T \{ J_\mu(x) J_\nu(0) \} | P(p) \rangle = \epsilon_{\mu\nu\alpha\beta} q_1^\alpha q_2^\beta \mathcal{F}_{p\gamma^*\gamma^*}(q_1^2, q_2^2), \quad (14)$$

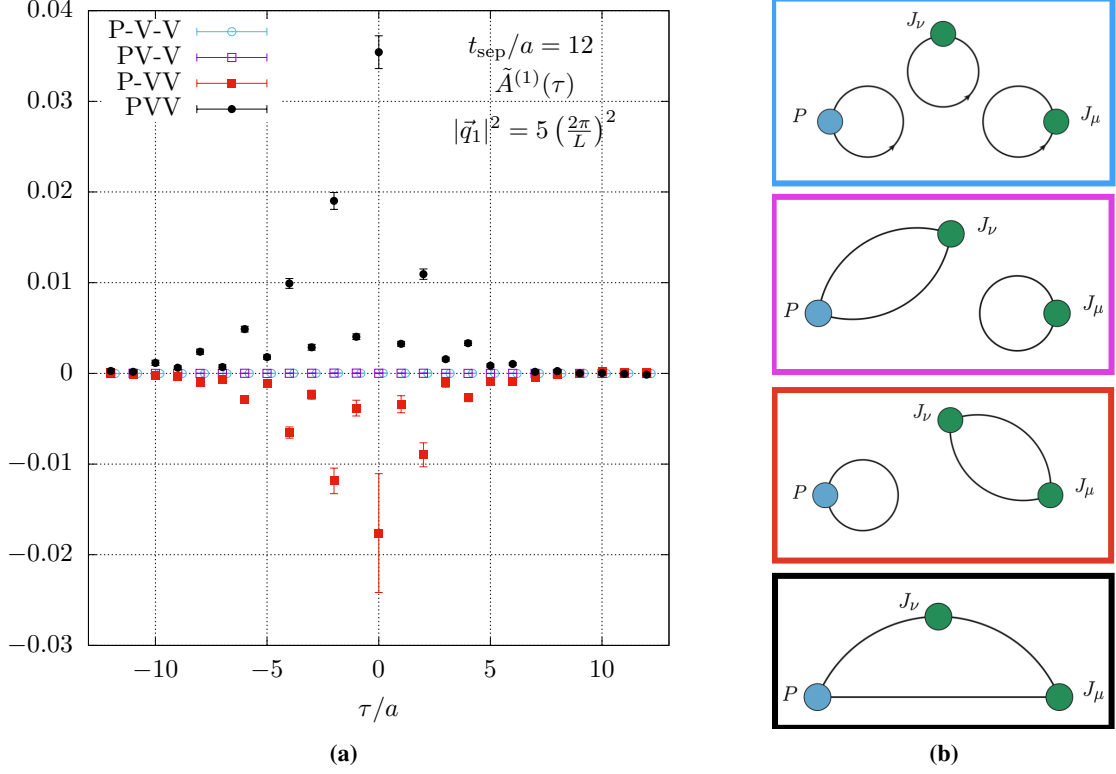


Figure 4: Left: The integrand of the η_8 TFF for specified kinematic condition; t_{sep} refers to the separation between the pseudoscalar and one of the vector currents that is kept fixed. Right: Illustration of the different topologies of the connected and disconnected contributions to the three-point function.

where q_1 and q_2 are the photon 4-momenta, J_μ is the hadronic component of the electromagnetic current and $\epsilon_{\mu\nu\alpha\beta}$ is a 4-rank Levi Civita tensor. On the lattice, one can relate three-point functions to the Euclidean version of these matrix elements [28]. We write

$$M_{\mu\nu}^E = \frac{2E_P}{Z_P} \int_{-\infty}^{\infty} d\tau e^{\omega_1 \tau} \tilde{A}_{\mu\nu}(\tau),$$

where E_P and Z_P are respectively the pseudoscalar energy and overlap of the pseudoscalar state with the interpolating operator, ω_1 is a free parameter $q_1 = (\omega_1, \vec{q}_1)$, $q_2 = (E_P - \omega_1, \vec{q}_2)$, and

$$\tilde{A}_{\mu\nu}(\tau) \equiv \lim_{t_P \rightarrow \infty} e^{E_P(t_f - t_0)} C_{\mu\nu}^{(3)}(\tau, t_P),$$

$$C_{\mu\nu}^{(3)}(\tau, t_P) = a^6 \sum_{\vec{x}, \vec{z}} \langle J_\mu(\vec{z}, t_i) J_\nu(\vec{0}, t_f) P^\dagger(\vec{x}, t_0) \rangle e^{i\vec{p} \cdot \vec{x}} e^{-i\vec{q}_1 \cdot \vec{z}}.$$

Here we have defined $\tau = t_i - t_f$, the time-difference between the two vector currents and $t_P = \min(t_f - t_0, t_i - t_0)$, the minimal time separation between the pseudoscalar and the vector currents. In the three-point function, P is the interpolating operator for the pseudoscalar meson, expressed in terms of O_8 , O_0 and appropriate mixing parameters; J_μ is implemented using the conserved vector current which does not require renormalization [2]. Note also that, an accurate determination of the

mixing parameters and the masses of the η, η' mesons is important, as they enter in the three-point function.

$\tilde{A}_{\mu\nu}$ can be decomposed into two scalar functions $\tilde{A}^{(1)}, \tilde{A}^{(2)}$ that form the integrand of the TFF (for technical details we refer to [9]). In Figure 4, we show preliminary results for one of these scalar functions in the $\vec{p} = \vec{0}$ frame, where we focus on η_8 , thus discarding any mixing with η_0 . The latter is important, and will be implemented in the future. Note that four different topologies contribute to the integrand (the hyphen indicates a disconnection): the two dominant PVV connected and P-VV disconnected loops; and the negligible PV-V and P-V-V disconnected loops. The P-VV loop has a significant and negative contribution and therefore we observe a large cancellation with the PVV loop. As a consequence, a good control of the disconnected VV and P loops is important.

5. Conclusions

We have shown preliminary results toward the extraction of the η, η' mass using staggered quarks. Using the GEVP and several noise reduction techniques, we are able to obtain a good signal for the η and η' effective mass. Alongside this, we have shown promising preliminary results for the integrand of the TFF of the η_8 state. In this context we have found that the two leading contributions are the fully connected PVV and disconnected P-VV loops, while the disconnected PV-V and P-V-V loops are of a marginal size.

Presently, we are accumulating statistics for our P-VV contribution, to further reduce its error. At the same time, we will explore the signal of the η, η' and their TFFs, including therefore mixing between the states. We plan to do this on several lattice spacings and volumes, improving also the statistics on the different ensembles that we have already analyzed. Ultimately, we will perform a continuum extrapolation of the TFFs.

6. Acknowledgements

This publication received funding from the Excellence Initiative of Aix-Marseille University - A*MIDEX, a French “Investissements d’Avenir” programme, AMX-18-ACE-005 and from the French National Research Agency under the contract ANR-20-CE31-0016. Center de Calcul Intensif d’Aix-Marseille is acknowledged for granting access to its high performance computing resources.

References

- [1] T. Aoyama et al., *The anomalous magnetic moment of the muon in the Standard Model*, *Phys. Rept.* **887** (2020) 1 [2006.04822].
- [2] S. Borsanyi et al., *Leading hadronic contribution to the muon magnetic moment from lattice QCD*, *Nature* **593** (2021) 51 [2002.12347].
- [3] G. Colangelo, M. Hoferichter, M. Procura and P. Stoffer, *Dispersive approach to hadronic light-by-light scattering*, *JHEP* **09** (2014) 091 [1402.7081].
- [4] G. Colangelo, M. Hoferichter, B. Kubis, M. Procura and P. Stoffer, *Towards a data-driven analysis of hadronic light-by-light scattering*, *Phys. Lett. B* **738** (2014) 6 [1408.2517].
- [5] G. Colangelo, M. Hoferichter, M. Procura and P. Stoffer, *Dispersion relation for hadronic light-by-light scattering: theoretical foundations*, *JHEP* **09** (2015) 074 [1506.01386].

- [6] E.-H. Chao, R.J. Hudspith, A. Gérardin, J.R. Green, H.B. Meyer and K. Ottnad, *Hadronic light-by-light contribution to $(g - 2)_\mu$ from lattice QCD: a complete calculation*, *Eur. Phys. J. C* **81** (2021) 651 [2104.02632].
- [7] T. Blum, N. Christ, M. Hayakawa, T. Izubuchi, L. Jin, C. Jung et al., *Hadronic light-by-light scattering contribution to the muon anomalous magnetic moment from lattice QCD*, *Physical Review Letters* **124** (2020) .
- [8] A. Gérardin, H.B. Meyer and A. Nyffeler, *Lattice calculation of the pion transition form factor $\pi^0 \rightarrow \gamma^* \gamma^*$* , *Phys. Rev. D* **94** (2016) 074507 [1607.08174].
- [9] A. Gérardin, H.B. Meyer and A. Nyffeler, *Lattice calculation of the pion transition form factor with $N_f = 2 + 1$ Wilson quarks*, *Phys. Rev. D* **100** (2019) 034520 [1903.09471].
- [10] S. Burri, *Pseudoscalar-Photon Transition Form Factors from Twisted Mass Lattice QCD*, *Asia-Pacific Symposium for Lattice Field Theory (APLAT)* (2020) .
- [11] A. Gérardin, *The anomalous magnetic moment of the muon: status of Lattice QCD calculations*, *Eur. Phys. J. A* **57** (2021) 116 [2012.03931].
- [12] G.S. Bali, V. Braun, S. Collins, A. Schäfer and J. Simeth, *Masses and decay constants of the η and η' mesons from lattice QCD*, 2021.
- [13] ETM collaboration, *Flavor-singlet meson decay constants from $N_f = 2 + 1 + 1$ twisted mass lattice QCD*, *Phys. Rev. D* **97** (2018) 054508 [1710.07986].
- [14] G. 't Hooft, *Computation of the Quantum Effects Due to a Four-Dimensional Pseudoparticle*, *Phys. Rev. D* **14** (1976) 3432.
- [15] M. Creutz, *Why rooting fails*, *PoS LATTICE2007* (2007) 007 [0708.1295].
- [16] A.S. Kronfeld, *Lattice Gauge Theory with Staggered Fermions: How, Where, and Why (Not)*, *PoS LATTICE2007* (2007) 016 [0711.0699].
- [17] B. Blossier, M.D. Morte, G.v. Hippel, T. Mendes and R. Sommer, *On the generalized eigenvalue method for energies and matrix elements in lattice field theory*, *Journal of High Energy Physics* **2009** (2009) 094–094.
- [18] M.F.L. Golterman, *STAGGERED MESONS*, *Nucl. Phys. B* **273** (1986) 663.
- [19] MT(c) collaboration, *The Hadron spectrum in QCD with dynamical staggered fermions*, *Nucl. Phys. B* **389** (1993) 445.
- [20] G.W. Kilcup and S.R. Sharpe, *A Tool Kit for Staggered Fermions*, *Nucl. Phys. B* **283** (1987) 493.
- [21] L. Giusti, P. Hernandez, M. Laine, P. Weisz and H. Wittig, *Low-energy couplings of QCD from current correlators near the chiral limit*, *Journal of High Energy Physics* **2004** (2004) 013–013.
- [22] T. DeGrand and S. Schaefer, *Improving meson two-point functions by low-mode averaging*, *Nuclear Physics B - Proceedings Supplements* **140** (2005) 296–298.
- [23] G.S. Bali, S. Collins and A. Schäfer, *Effective noise reduction techniques for disconnected loops in lattice qcd*, *Computer Physics Communications* **181** (2010) 1570–1583.
- [24] T. Blum, T. Izubuchi and E. Shintani, *New class of variance-reduction techniques using lattice symmetries*, *Physical Review D* **88** (2013) .
- [25] L. Venkataraman and G. Kilcup, *The eta-prime meson with staggered fermions*, [hep-lat/9711006](https://arxiv.org/abs/hep-lat/9711006).
- [26] C. Michael, K. Ottnad and C. Urbach, *η and η' mixing from lattice QCD*, *Physical Review Letters* **111** (2013) .
- [27] S. Aoki, H. Fukaya, S. Hashimoto and T. Onogi, *Finite volume QCD at fixed topological charge*, *Physical Review D* **76** (2007) .
- [28] X. Ji and C. Jung, *Studying hadronic structure of the photon in lattice QCD*, *Physical Review Letters* **86** (2001) 208–211.